Inorganic Nanotubes

G. R. Patzke, F. Krumeich, R. Nesper,
Angew. Chem. Int.Ed. Engl. 14 (2002) 2447

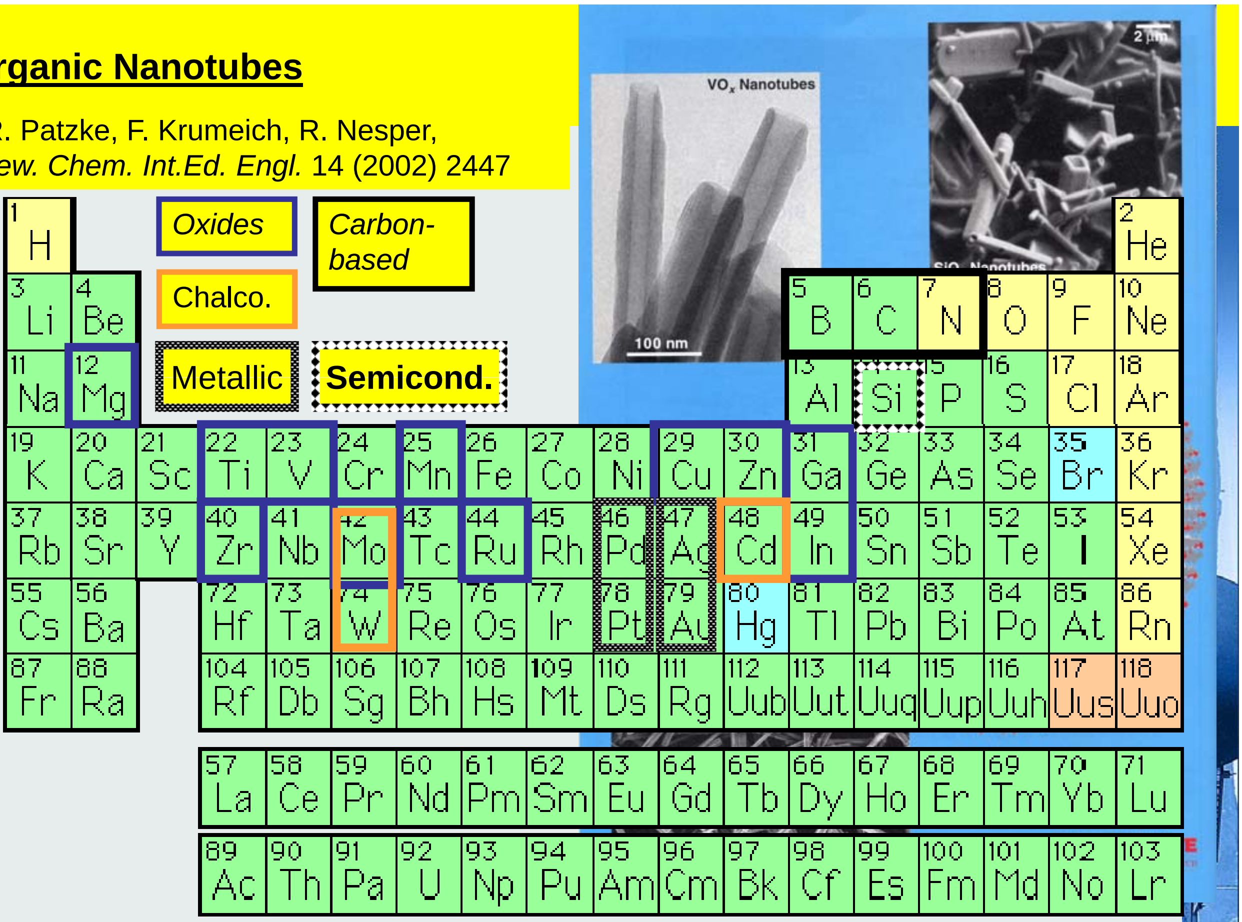

History

Tubular Silicate minerals

TEM investigation of the cross-sections of Chrysotile

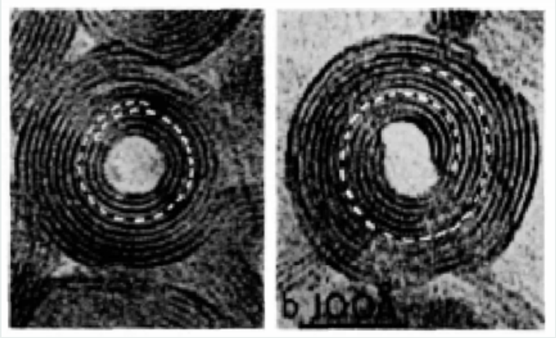

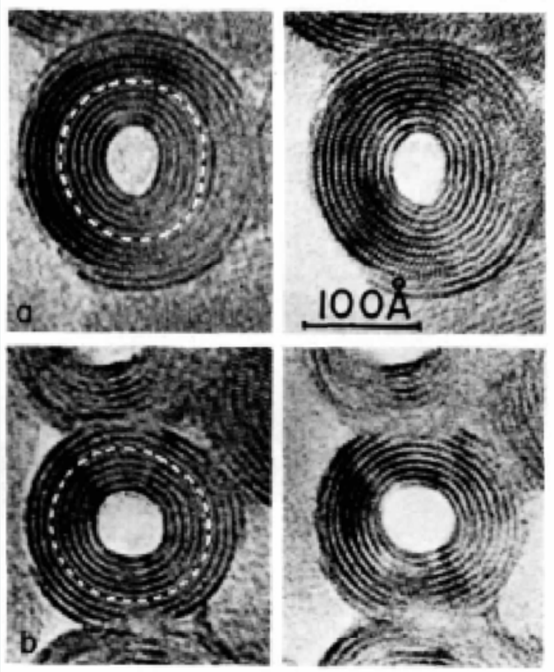

Scrolls of one or more layers

<u>But</u>: also closed, concentric cylinders

Yada, *Acta Crystallogr. A* **27** (1971) 659

Nanotubes

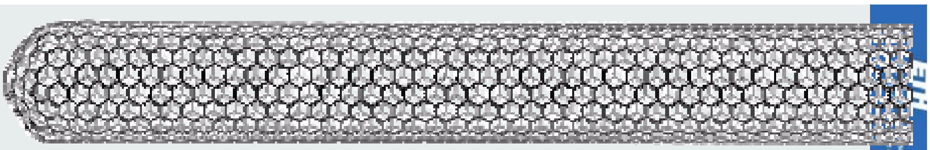

CRYSOTILE, Bi-Nb-S

carbon	
boron nitride	(BN, $B_xC_yN_z$)
boron carbide	(B_xC)
silicon dioxide	**(amorphous)**
transition metal oxide	**(VO_x, TiO_2)**
metal sulfide	**(MoS_2, WS_2, NbS_2, InS, $CdS(e)$)**
transition metal halide	**($NiCl_2$)**
metal	**(Au, Ni, Bi, Te)**

BN Nanotubes

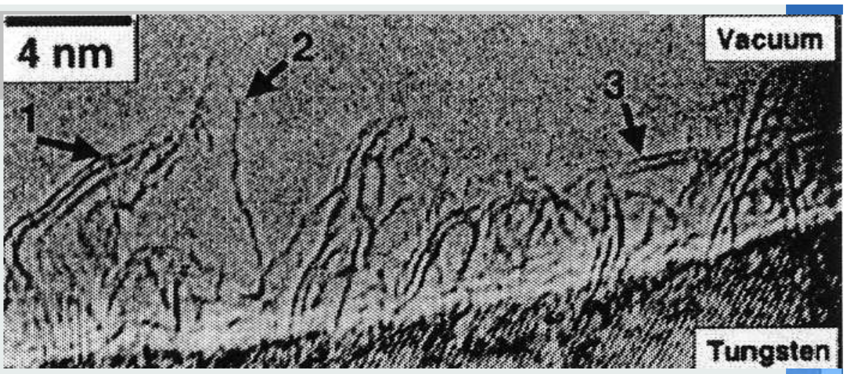

Fig. 36 HREM image of single-walled BN nanotubes adhering on a W substrate. (Reproduced with permission from ref. 110).

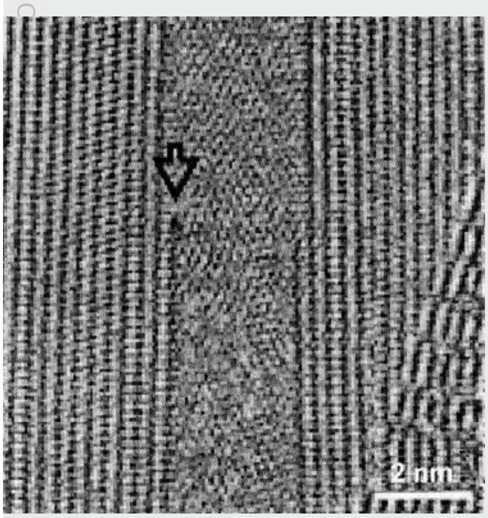

BN Nanotubes

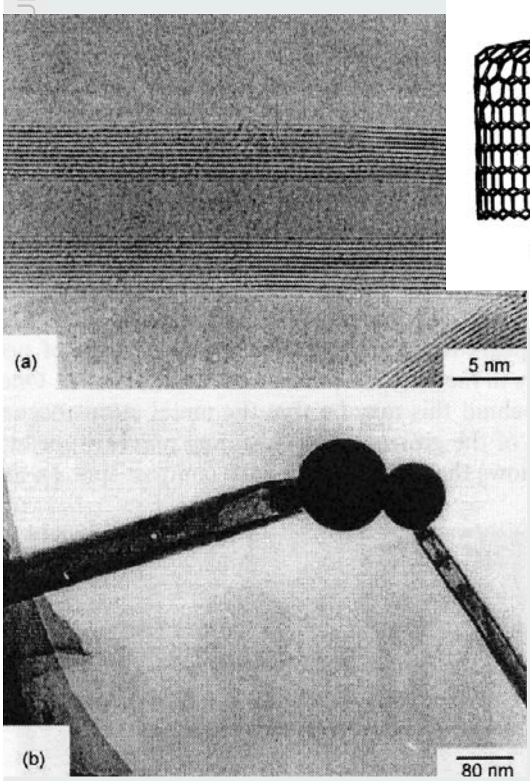

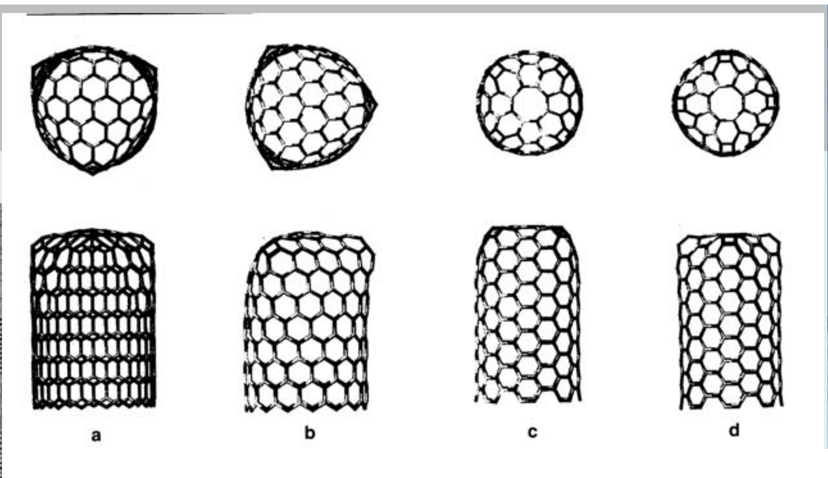

BC$_x$ Nanotubes

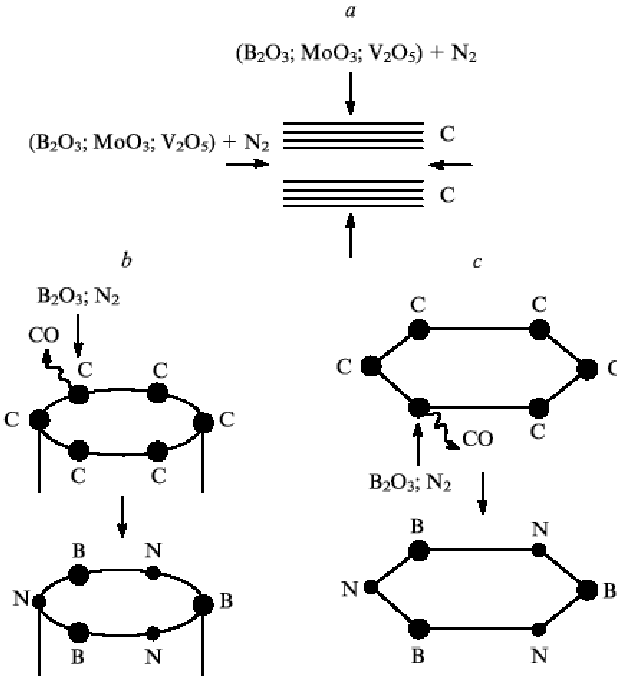

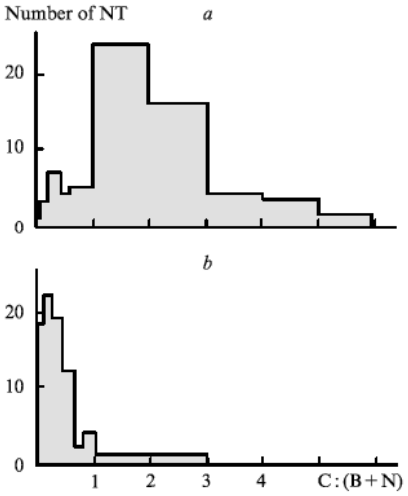

Figure 3. Composition histogram of multilayer BCN-nanotubulenes synthesised by chemical substitution from carbon NT (at 1773 K in a flow of nitrogen);[63]
(*a*) without oxides, (*b*) in the presence of MoO$_2$.

B-C-N Nanotubes

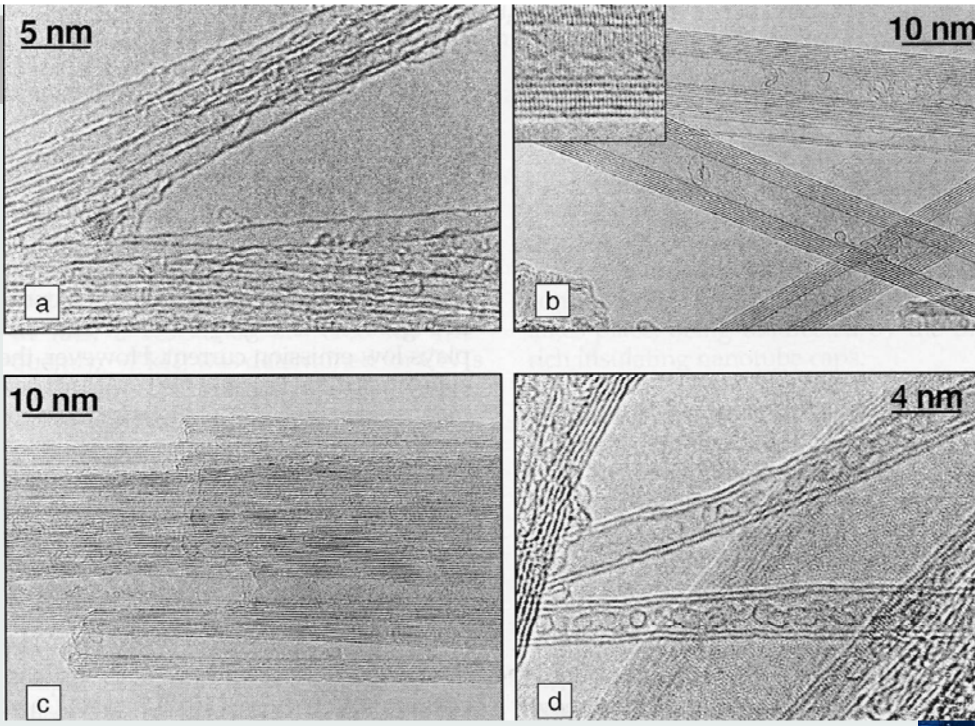

Figure 1. High-resolution transmission electron microscopy (TEM) images of B-C-N nanotubes converted from carbon nanotubes (CNTs) by means of high-temperature chemical reactions:[16–22] *(a) B/N-doped C single-walled nanotube bundles; (b) BN-rich multiwalled B-C-N nanotubes; (c) ropes made of dozens of open-ended BN-rich B-C-N nanotubes; and (d) double-walled BN-rich B-C-N nanotubes with C buckyballs in their cores. Inset in (b) shows a high-resolution TEM micrograph of a BN-rich B-C-N multiwalled nanotube wall fragment exhibiting atom column separation of ~0.21 nm along the shells; this is peculiar to "zigzag"-oriented shells (tube axis parallel to the* $[10\bar{1}0]$ *orientation of a graphitic sheet).*

B-C-N Nanotubes

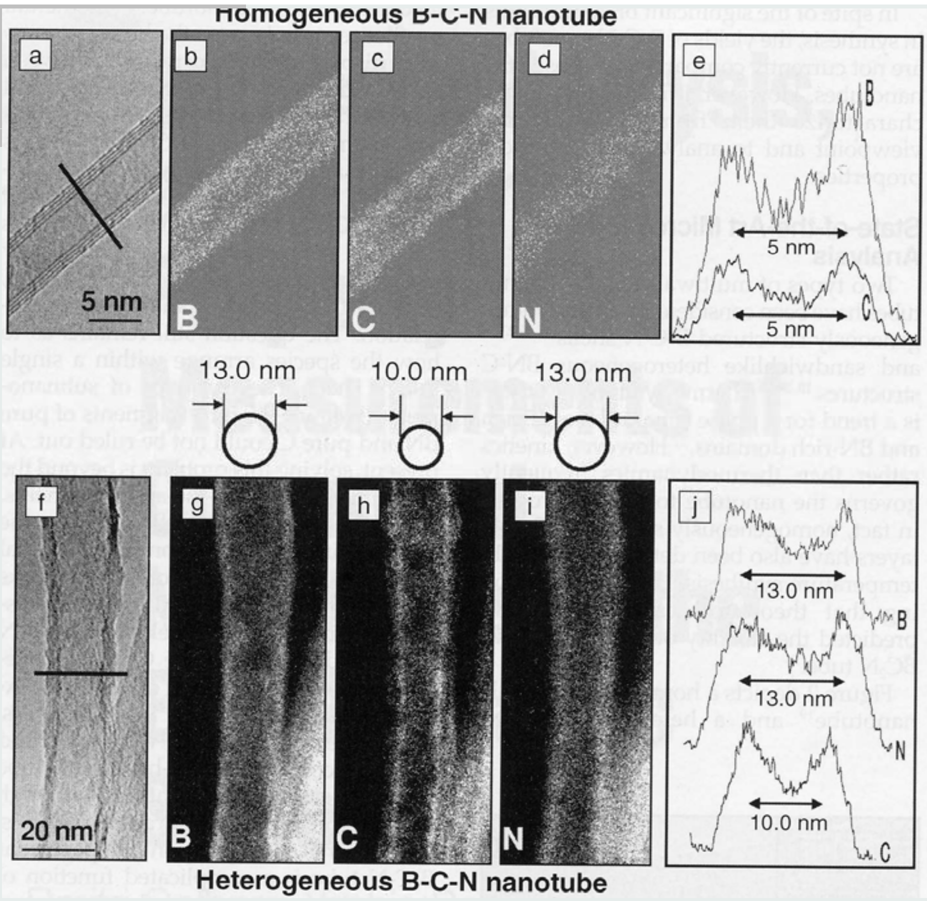

Nanotubes of Dichalcogenides– MoX_2

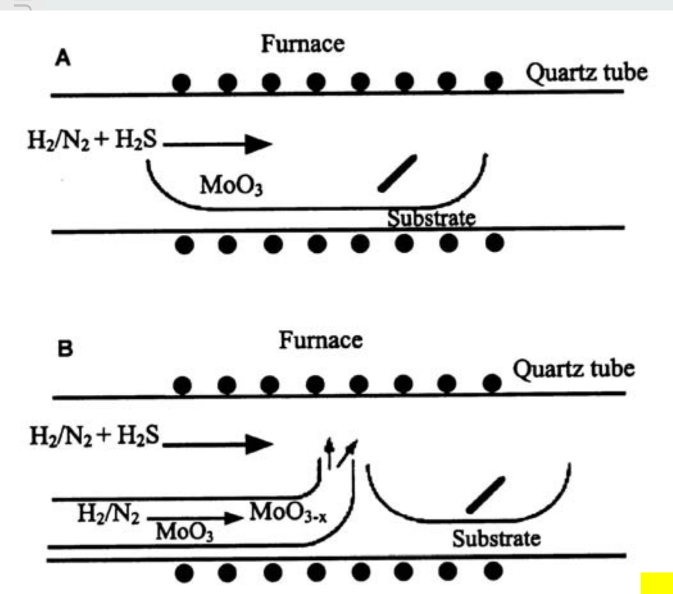

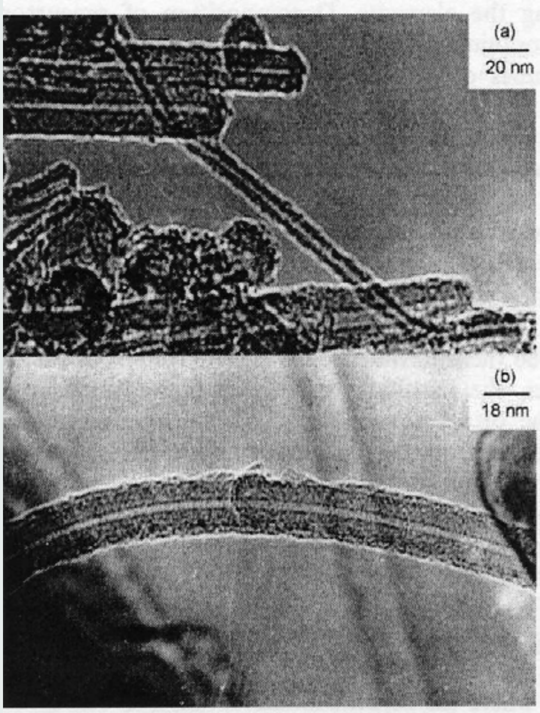

Tenne, Margulis, Genut, Hodes, *Nature* 360 (1992) 444

Nanotubes of Layered Materials

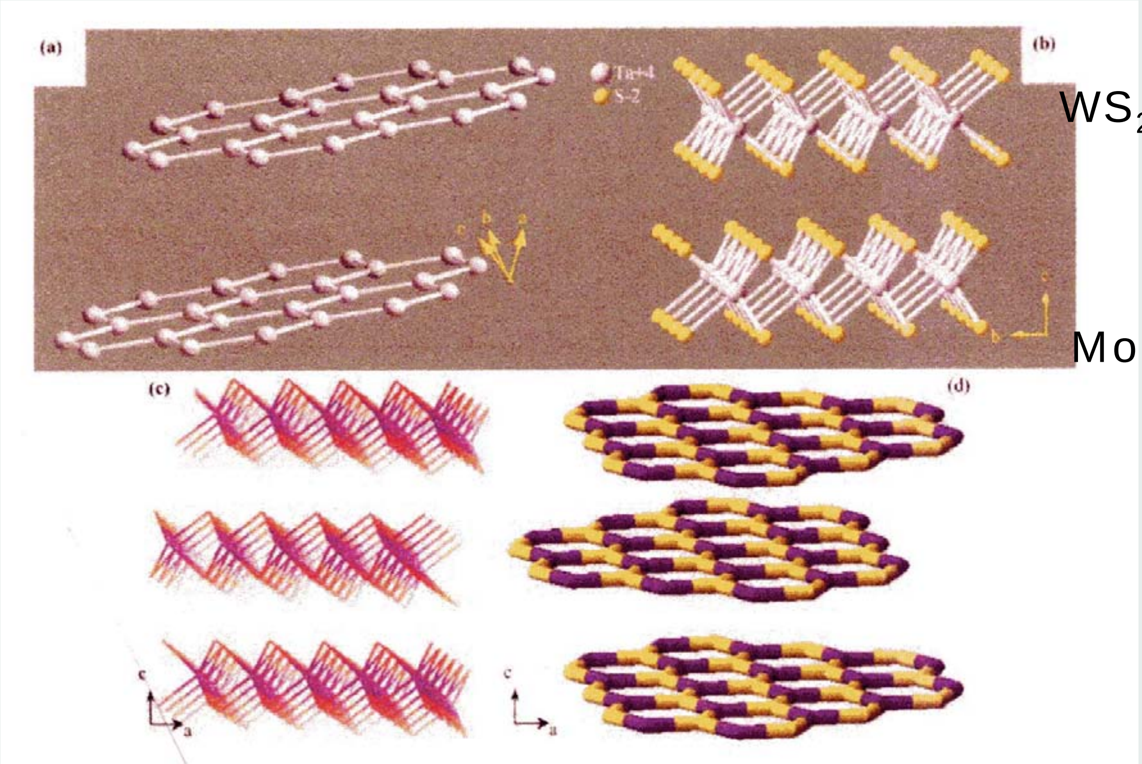

WS_2

MoS_2

Nanotubes of Dichalcogenides– MoX_2

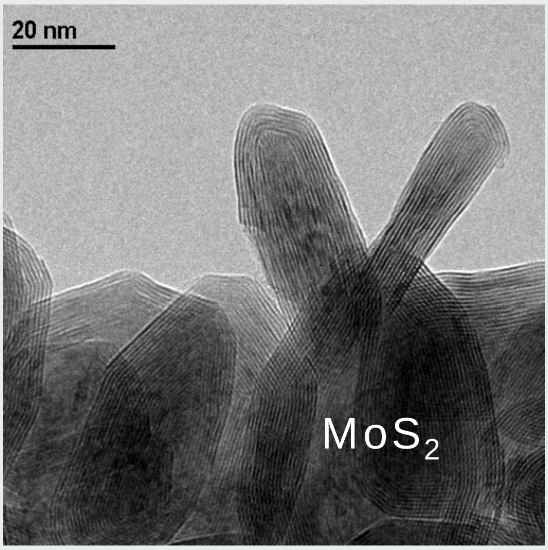

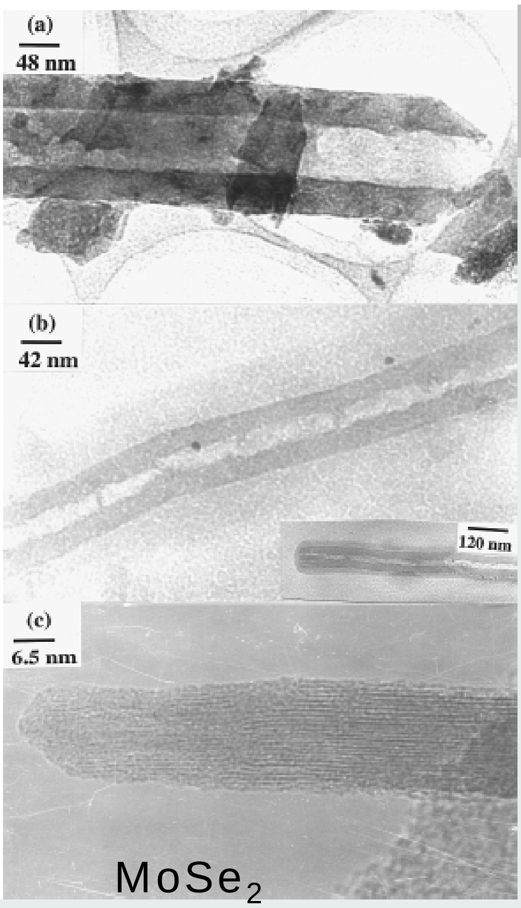

Tenne, Margulis, Genut, Hodes, *Nature* 360 (1992) 444

***C.N.R. Rao et al, Chem. Commun.*, 2001, 2236–2237**

Nanotubes of Dichalcogenides– WX_2

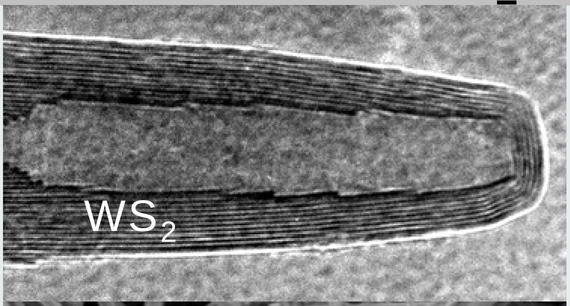

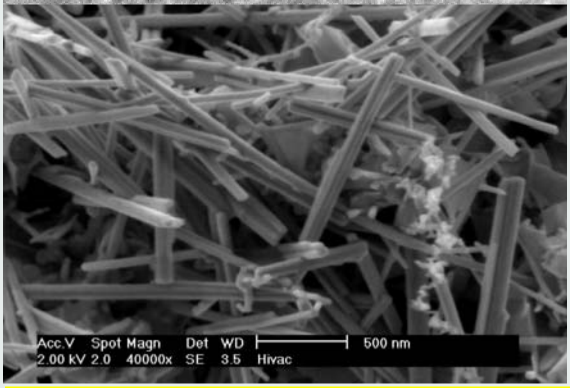

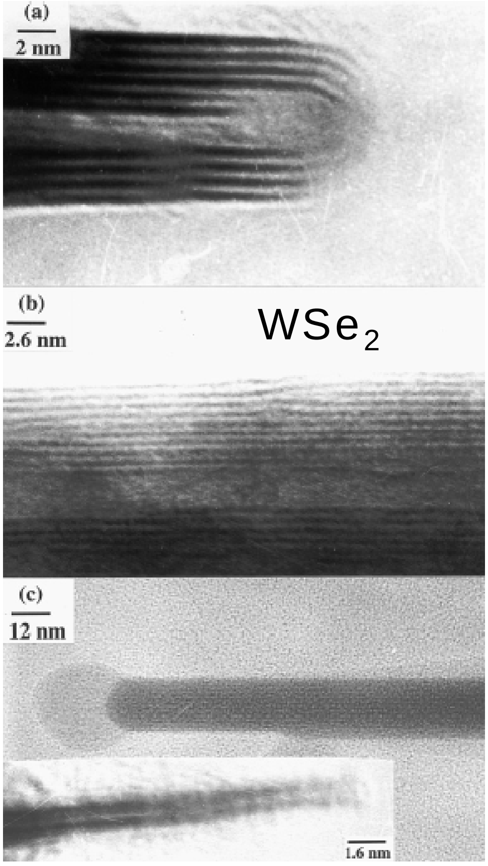

Tenne, Margulis, Genut, Hodes, *Nature* 360 (1992) 444

***C.N.R. Rao et al, Chem. Commun.*, 2001, 2236–2237**

Nanotubes of Dichalcogenides– W/Nb/X_y

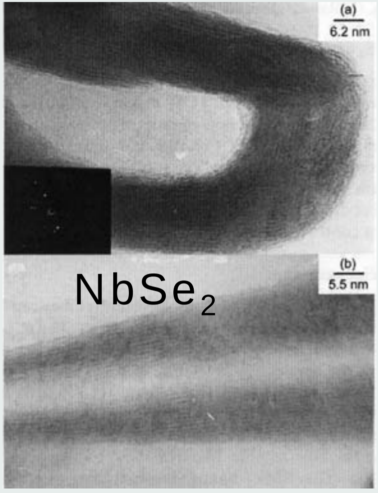

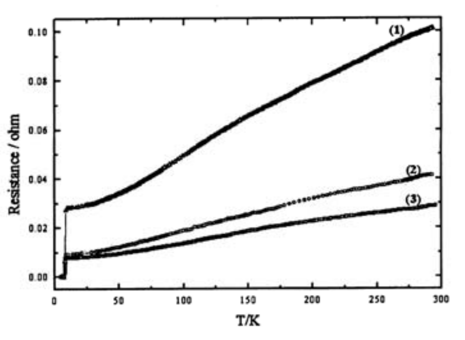

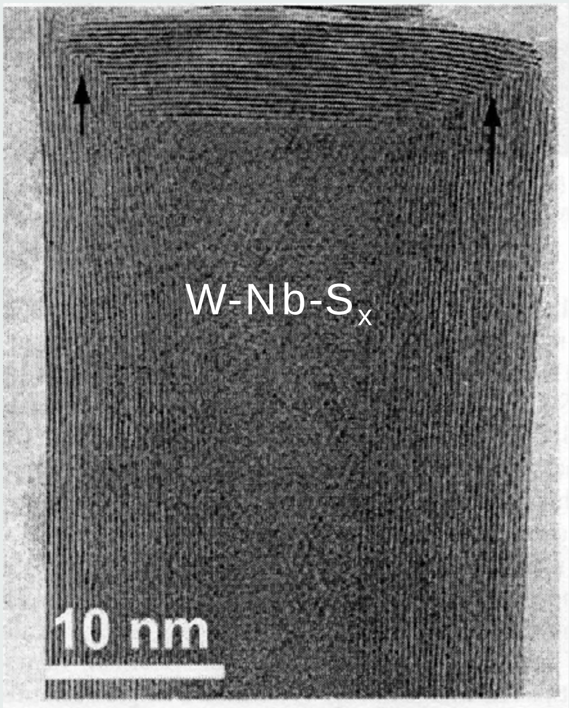

Fig. 18 TEM image showing the sharp 90° bend observed in the W–Nb–S nanotubes. (Reproduced with permission from ref. 41*a*).

Nanotubes of Dichalcogenides– ReS_2

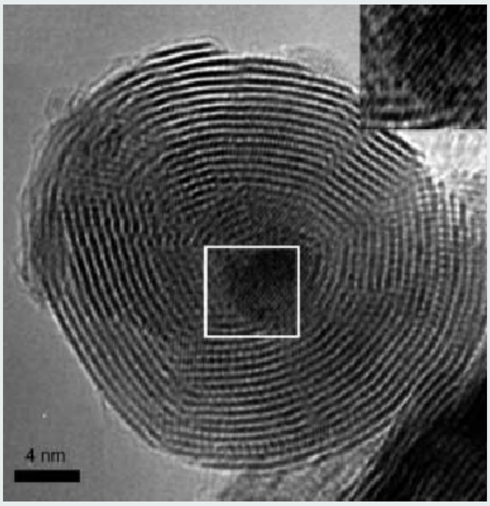

Abbildung 5. HRTEM-Aufnahme eines kleinen ReS_2-Partikels, in das ein ReO_2-Nanopartikel eingeschlossen ist. Die 0.29 nm breiten Gitterstreifen (Einschub) entsprechen den ReO_2-{111}-Ebenen.

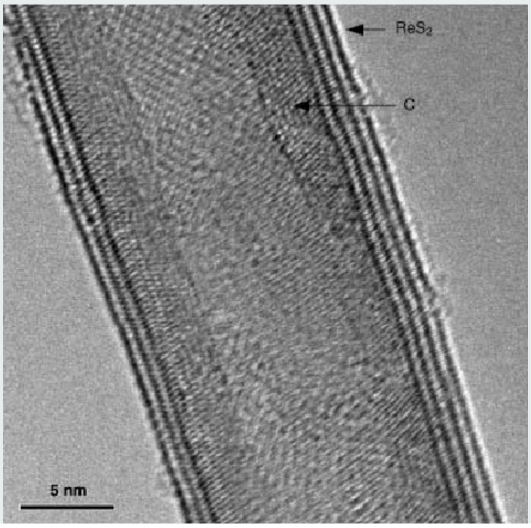

Abbildung 6. HRTEM-Aufnahme einer ReS_2-Nanoröhre, die auf einer MWCNT als Templat gewachsen ist. Die ReS_2-Röhrenwände sieht man als sehr dunkle parallele Linien mit relativ großen Abständen dazwischen. Die Kohlenstoffwände der darunter liegenden MWCNT sind weniger deutlich zu erkennen, und die Abstände zwischen ihnen sind sehr viel geringer.

Nanotube Tips of Dichalcogenides– WX_2

Fig. 16 Various closed tips observed in WS_2 tubes possibly containing square or octagonal defects. (Reproduced with permission from ref. 47).

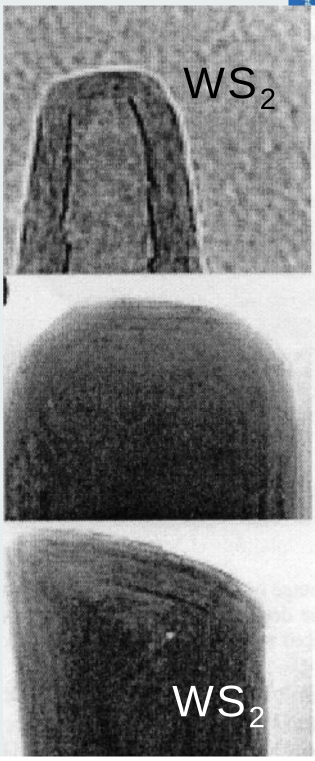

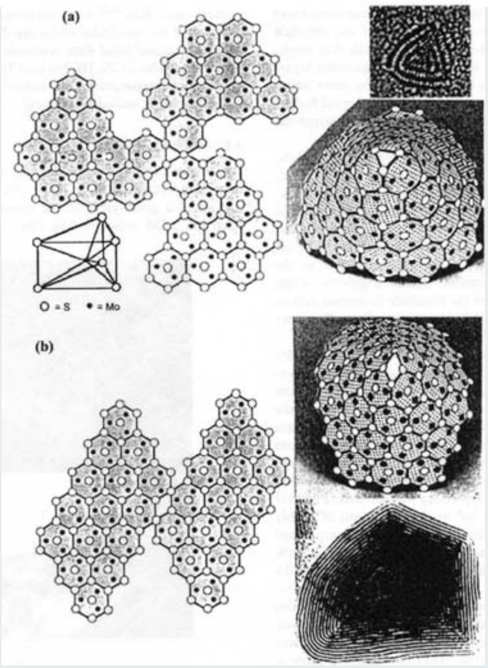

Fig. 17 Illustration of various point defects which exists in the vertices of IF MoS_2: (a) a triangular point defect; (b) a rhombohedral point defect. Insets show IF structures that are likely to contain such point defects. (Reproduced with permission from ref. 19).

“TiO_2” Nanotubes

Kasuga, Hiramatsu, Hoson, Sekino, Niihara,
***Langmuir* 14, (1998) 3160**

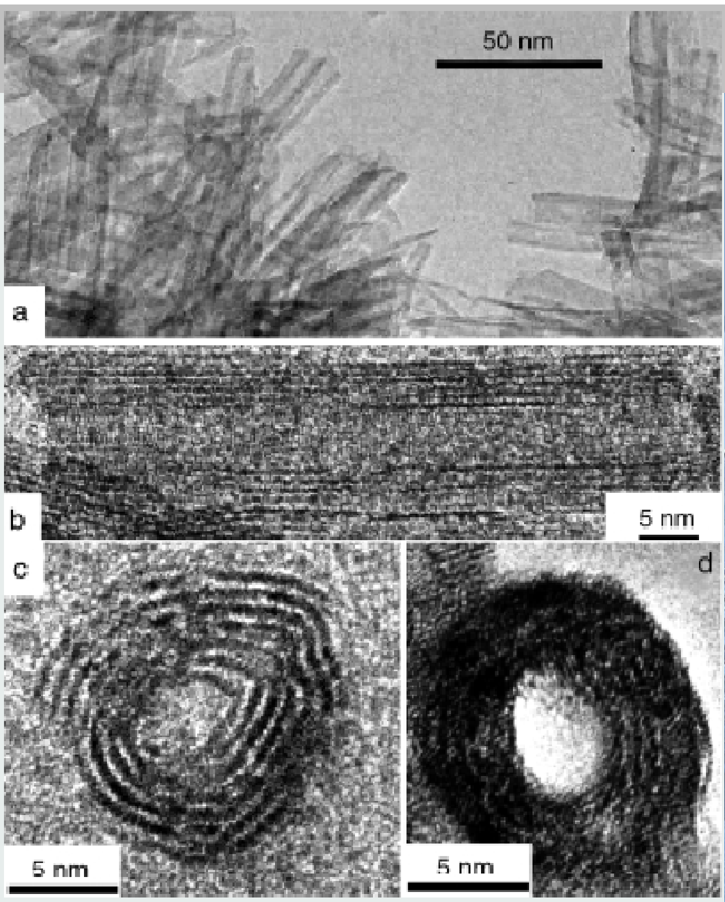

“TiO_2” Nanotubes

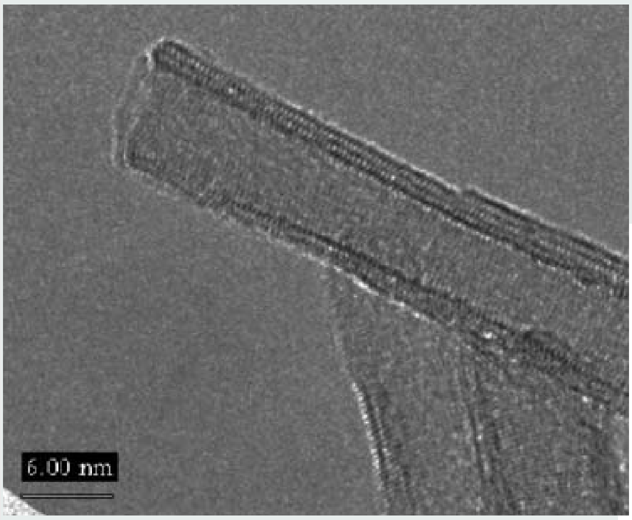

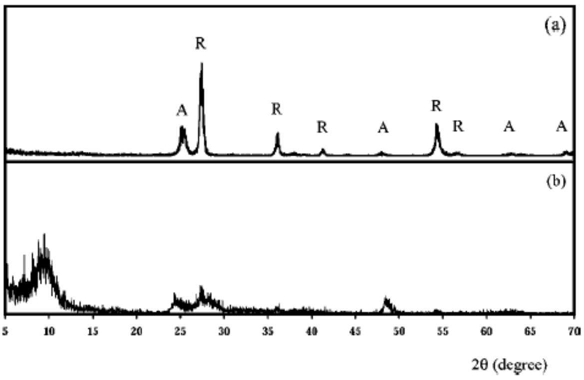

FIG. 4. XRD profiles taken from (a) a TiO_2 sample formed by sol-gel procedure and (b) titanium oxide nanotubes (sample B). In (a) peaks resulting from the anatase phase are denoted by A and those from the rutile phase are denoted by R.

G. H. Du, Q. Chen, R. C. Che, Z. Y. Yuan, L.-M. Peng, **APPLIED PHYSICS LETTERS VOLUME 79 (2001) 3702**

$NiCl_2$ Nanotubes

Y. R. Hacohen, E. Grunbaum, R. Tenne, J. Sloan, J. L. Hutchison, Nature (London) 395 336 (1998)

$CdCl_2$ structure types !

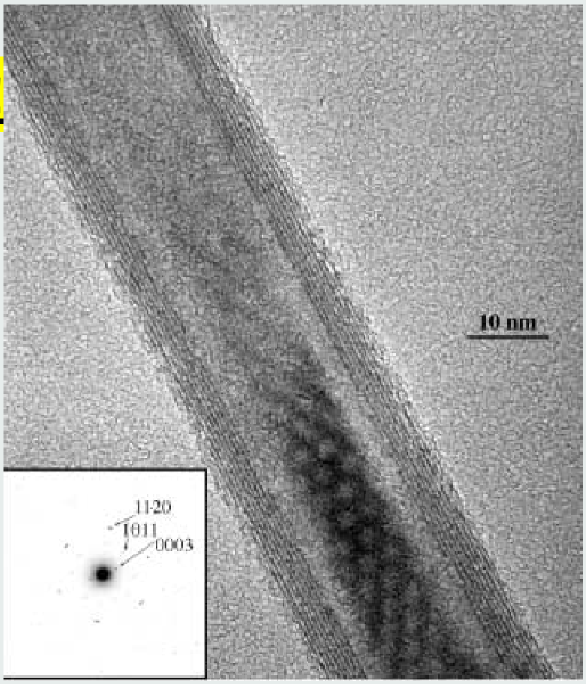

Multilayer NT were obtained; their cross-sections were up to ~7 nm, while the lengths were several micrometres.

The tubular structures remained stable for a few days. It is assumed 136 that the most interesting applications of such structures may be related to their unusual magnetic characteristics.

It should be noted that it is compounds which form phases with quasi-2D structures under equilibrium conditions that are usually considered as potential candidates for the synthesis of NT.

$Tb(OH)_3$, Tb_4O_7, $Y(OH)_3$, and Y_2O_3 nanotubes

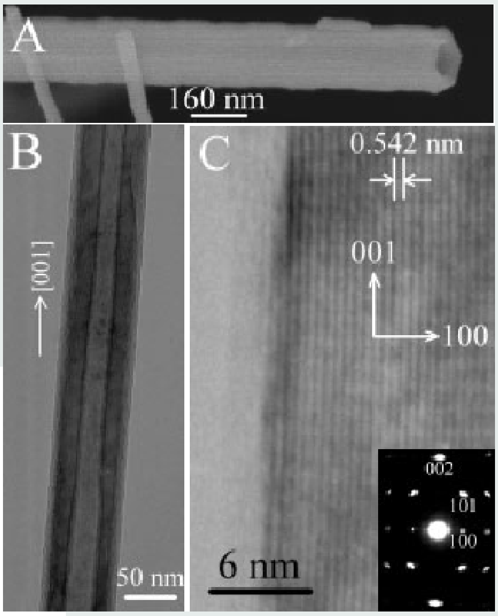

Fig. 7. A) An SEM image of the as-synthesized $Y(OH)_3$ product. B) TEM image of a single $Y(OH)_3$ nanotube. C) An HRTEM image of the outside part of the tube wall, clearly showing resolved fringes of (100) planes (spacing $d = 0.542$ nm). Inset: The SAED pattern recorded from the [010] zone axis.

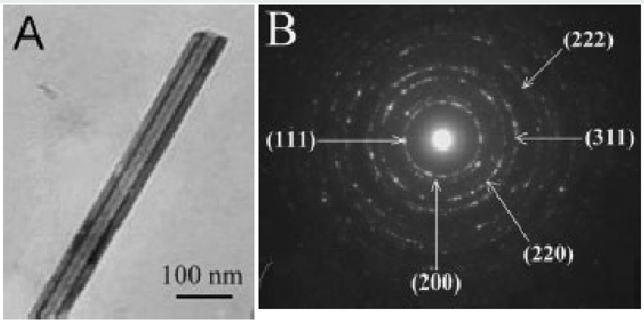

Fig. 5. A) A typical TEM image of a single Tb_4O_7 nanotube. The Tb_4O_7 product was obtained by calcination of the as-synthesized $Tb(OH)_3$ at 450°C for 6 h in air. B) ED pattern of the Tb_4O_7 nanotubes.

Helical Mesostructured Tubules from Taylor Vortex-Assisted Surfactant Templates**

Adv. Mater. **2001**, *13*, No. 15, August 3

By *Won-Jong Kim* and *Seung-Man Yang**

Schematic illustration of the coil-spring flow between a stationary outer cylinder and a rotating inner cylinder. The two cylinders are aligned coaxially. The inner and outer cylinders are 10 cm in length, and 4 and 4.4 cm in radius, respectively.

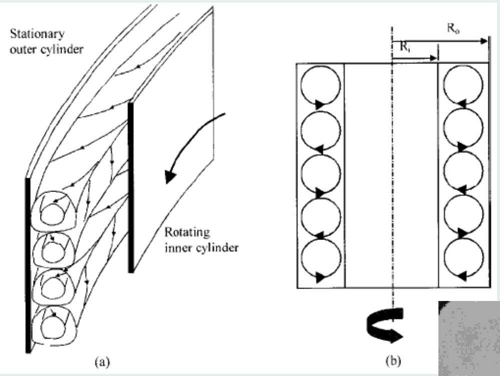

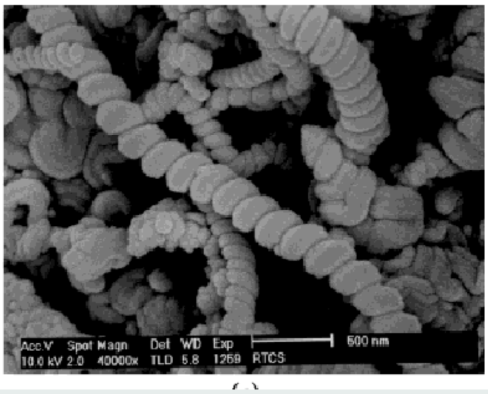

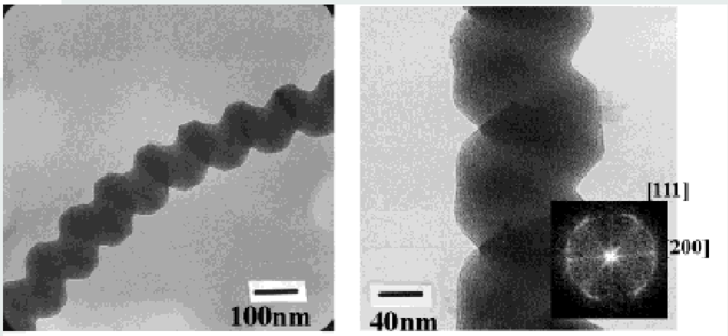

Synthesis: Cetyltrimethylammonium bromide (CTAB: Sigma) and sodium salicylate (NaSal: Aldrich) were used to prepare the wormlike micelles, which served as the template. Tetraethylorthosilane (TEOS: Aldrich) in hydrochloric acid (HCl: Junsei) was used as a precursor of the silica substrate used to form the silica±surfactant meso-structure.

Noble-Metal Nanotubes (Pt, Pd, Ag) from Lyotropic Mixed-Surfactant Liquid-Crystal Templates**

Tsuyoshi Kijima, Takumi Yoshimura, Masafumi Uota, Takayuki Ikeda, Daisuke Fujikawa, Shinji Mouri, and Shinji Uoyama*

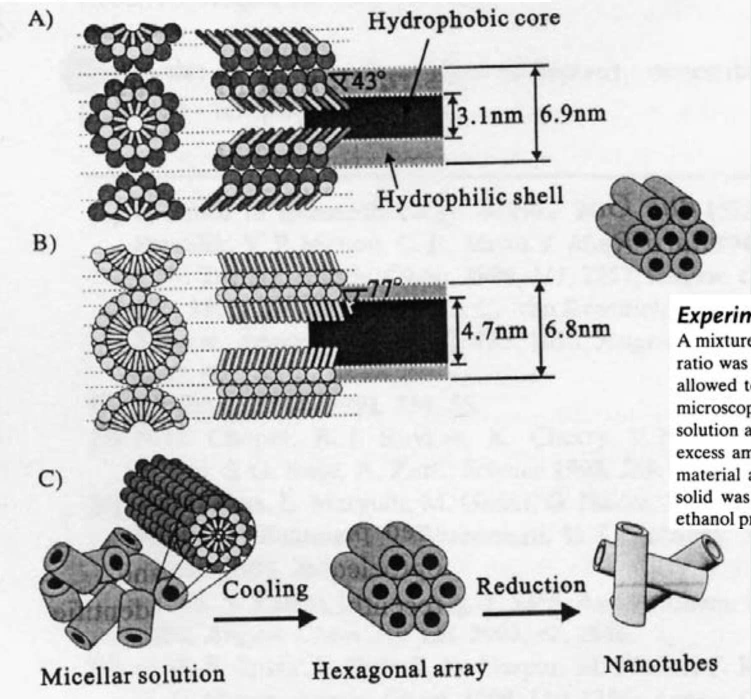

Figure 4. Schematic models for the formation of platinum nanotubes in the mixed surfactant templating system: A) Mixed ($C_{12}EO_9$/Tween 60) and B) single ($C_{12}EO_9$) surfactant cylindrical rodlike micelles. C) Pathway from micellar solution to metal nanotubes by the reduction of metals salts confined to the aqueous shell of mixed-surfactant cylindrical micelles. The metal salts and water molecules are omitted from the models.

Experimental Section

A mixture of H_2PtCl_6, $C_{12}EO_9$, Tween 60, and H_2O in a 1:1:1:60 molar ratio was shaken at 60°C, then cooled to between 15 and 25°C and allowed to stand at that temperature for 30 min. Polarizing optical microscopy revealed that the homogeneous mixture was an isotropic solution at 60°C and transformed around 28°C into a LC phase. An excess amount of hydrazine was added to the cooled (25°C) pasty material and then kept at that temperature for 24 h. The resulting solid was separated, washed with water and then repeatedly with ethanol prior to drying in air. Similar syntheses by using $Pd(NO_3)_2$, or

---

Semiconductor Nanotubes

NATURE |VOL 422 | 10 APRIL 2003

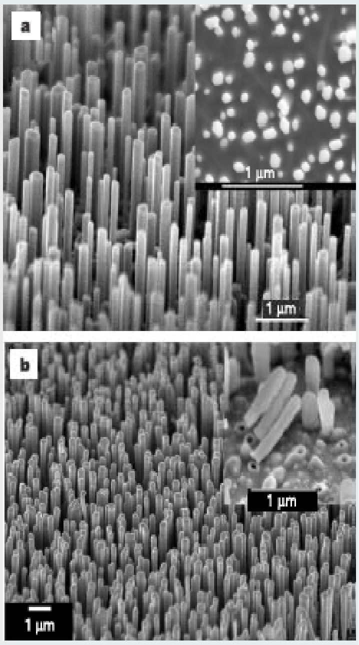

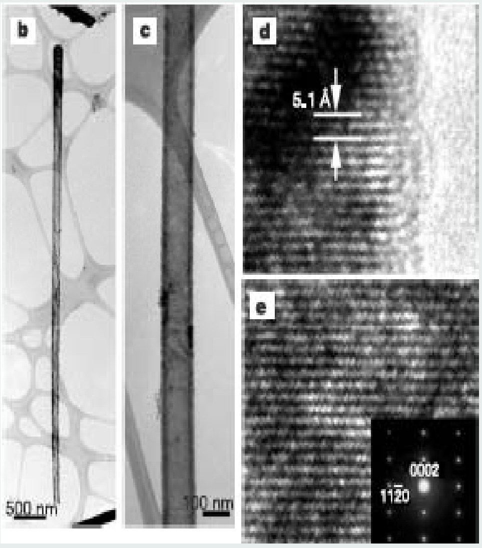

Semiconductor Nanotubes

Physica E 13 (2002) 969 – 973